Effects of Intratumoral Inflammatory Process on ^{18}F-FDG Uptake: Pathologic and Comparative Study with ^{18}F-Fluoro-α-Methyltyrosine PET/CT in Oral Squamous Cell Carcinoma

Mai Kim[1,2], Arifudin Achmad[2–4], Tetsuya Higuchi[2], Yukiko Arisaka[2], Hideaki Yokoo[5], Satoshi Yokoo[1], and Yoshito Tsushima[2]

[1]Department of Stomatology and Maxillofacial Surgery, Gunma University Graduate School of Medicine, Maebashi, Gunma, Japan; [2]Department of Diagnostic Radiology and Nuclear Medicine, Gunma University Graduate School of Medicine, Maebashi, Gunma, Japan; [3]Human Resource Cultivation Center, Gunma University, Kiryu, Gunma, Japan; [4]Department of Radiology, Faculty of Medicine, Gadjah Mada University, Yogyakarta, Indonesia; and [5]Department of Human Pathology, Gunma University Graduate School of Medicine, Maebashi, Gunma, Japan

The accurate depiction of both biologic and anatomic profiles of tumors has long been a challenge in PET imaging. An inflammation, which is innate in the carcinogenesis of oral squamous cell carcinoma (OSCC), frequently complicates the image analysis because of the limitations of ^{18}F-FDG and maximum standardized uptake values (SUV_{max}). New PET parameters, metabolic tumor volume (MTV) and total lesion glycolysis (TLG), as well as ^{18}F-fluoro-α-methyltyrosine (^{18}F-FAMT), a malignancy-specific amino acid–based PET radiotracer, are considered more comprehensive in tumor image analysis. Here, we showed the substantial effects of the intratumoral inflammatory process on ^{18}F-FDG uptake and further study the possibility of MTV and TLG to predict both tumor biology (proliferation activity) and anatomy (pathologic tumor volume). **Methods:** ^{18}F-FDG and ^{18}F-FAMT PET images from 25 OSCC patients were analyzed. SUV_{max} on the tumor site was obtained. PET volume computerized-assisted reporting was used to generate a volume of interest to obtain MTV and TLG for ^{18}F-FDG and total lesion retention (TLR) for ^{18}F-FAMT. The whole tumor dissected from surgery was measured and sectioned for pathologic analysis of tumor inflammation grade and Ki-67 labeling index. **Results:** The high SUV_{max} of ^{18}F-FDG was related to the high inflammation grade. The SUV_{max} ratio of ^{18}F-FDG to ^{18}F-FAMT was higher in inflammatory tumors ($P < 0.05$) whereas the corresponding value in tumors with a low inflammation grade was kept low. All ^{18}F-FAMT parameters were correlated with Ki-67 labeling index ($P < 0.01$). Pathologic tumor volume predicted from MTV of ^{18}F-FAMT was more accurate ($R = 0.90$, bias = 3.4 ± 6.42 cm^3, 95% confidence interval = 0.77–6.09 cm^3) than that of ^{18}F-FDG ($R = 0.77$, bias = 8.1 ± 11.17 cm^3, 95% confidence interval = 3.45–12.67 cm^3). **Conclusion:** ^{18}F-FDG uptake was overestimated by additional uptake related to the intratumoral inflammatory process, whereas ^{18}F-FAMT simply accumulated in tumors according to tumor activity as evaluated by Ki-67 labeling index in OSCC.

Key Words: inflammation; MTV; OSCC; ^{18}F-FAMT; ^{18}F-FDG

J Nucl Med 2015; 56:16–21
DOI: 10.2967/jnumed.114.144014

A worldwide estimation of newly diagnosed oral cavity cancer in 2008 was more than 250,000, with an estimated mortality number reaching 128,000 (*1*). Ninety percent of oral cavity cancer is oral squamous cell carcinoma (OSCC) derived from mucosal lining (*2*), which is directly exposed to the external environment. Despite the advancement of diagnostic imaging and detection of biologic markers, no significant improvement in survival rate was obtained over the past 40 y (*3*).

OSCC PET imaging using ^{18}F-FDG and maximum standardized uptake value (SUV_{max}) assessment is helpful for pretreatment staging and improved TNM classification (*4,5*). Even though it has been considered as an independent prognostic factor (*6*), the shortcoming of semiquantitative SUV_{max} is its dependency on a mere single pixel (*7*), which may not represent the whole tumor entity (*8*). Moreover, several major limitations of the standardized uptake value (SUV) concept affect its reliability as a surrogate of the targeted quantity, the metabolic rate of ^{18}F-FDG (*9*).

Because ^{18}F-FDG accumulation in tumor cells depends on glucose metabolism, PET is a sensitive modality for malignancy but lacks the specificity and ability to depict the true tumor biology. To address this, the amino acid–based PET radiotracer ^{18}F-fluoro-α-methyltyrosine (^{18}F-FAMT), which accumulates exclusively in malignant tumor cells through the L-type amino acid transporter 1, was developed (*10–12*). In previous OSCC studies, ^{18}F-FAMT was better than ^{18}F-FDG in its correlation with tumor proliferation activity, represented by Ki-67 labeling index (Ki-67 LI) (*13,14*). Moreover, significant false-positive accumulation of ^{18}F-FDG in inflammatory lesions, other nonmalignant lesions, and some normal organs due to physiologic activity contributes to the lower specificity of ^{18}F-FDG for malignancy.

Recently, metabolic tumor volume (MTV) and total lesion glycolysis (TLG), which quantify both anatomic and pathophysiologic aspects of the entire tumor, have been introduced as new

Received Nov. 3, 2014; revision accepted Nov. 4, 2014.
For correspondence or reprints contact: Mai Kim, Department of Stomatology and Maxillofacial Surgery, Gunma University Graduate School of Medicine; 3-39-22 Showa-machi, Maebashi, Gunma 371-8511, Japan.
E-mail: kimmu@gunma-u.ac.jp
Published online Dec. 4, 2014.

TABLE 1
Tumor Inflammation Grade

Grade	Interpretation
0	No inflammatory cells were present.
1	Inflammatory cells are visible at the invasive margin, however, invading cancer cell islets remain intact.
2	Inflammatory cells spread within the tumor area, with some destruction of invading cancer islets.
3	Very prominent inflammatory reaction within the tumor, with frequent destruction of cancer islets. Inflammatory cells also found beyond the tumor border.

evaluation parameters in ^{18}F-FDG PET and used as independent prognostic biomarkers in various solid malignancies (*15–17*). The addition of these new biomarkers into American Joint Committee on Cancer stage may provide more reliable outcome prediction in oral cancer patients (*18*).

^{18}F-FAMT discriminates malignant tumors from benign lesions in oral malignancies (*14,19*). Moreover, in OSCC, ^{18}F-FAMT provides more accurate assessment of bone marrow invasion than ^{18}F-FDG (*10*). In this study, we investigated how ^{18}F-FDG and ^{18}F-FAMT PET parameters (SUV_{max}, MTV, and TLG or total lesion retention [TLR]) might be affected by intratumoral inflammatory process through a study with tumor inflammation grade obtained from post-surgical specimen pathologic examination.

MATERIALS AND METHODS

Patients

The study involved 25 OSCC patients (11 men and 14 women; age, 31–88 y; mean age, 61.9 y) who were referred for surgery from April 2008 to March 2013. All patients underwent surgery after ^{18}F-FDG and ^{18}F-FAMT PET/CT imaging. The study protocol was approved by the institutional review board of Gunma University, and all patients who agreed to participate in the study signed a written informed consent form.

Radiopharmaceuticals and PET Image Analysis

^{18}F-FAMT and ^{18}F-FDG were produced in our hospital cyclotron facility. ^{18}F-FAMT was synthesized by the method developed by

TABLE 2
Characteristic of Patients and Tumors

				^{18}F-FDG parameters			^{18}F-FAMT parameters			^{18}F-FDG to ^{18}F-FAMT					
Patient no.	Age (y)/sex	Primary tumor origin	Stage	SUV_{max}	MTV	TLG	SUV_{max}	MTV	TLR	SUV_{max} ratio	MTV ratio	TLG-to-TLR ratio	Inflammation grade	Ki-67 LI	PTV (cm^3)
1	61/F	Tongue	I	5.2	8.8	28.9	3.4	3.6	7.3	1.5	2.4	4.0	1	41.7	0.6
2	88/F	Maxilla	IVa	12.2	15.8	85.4	1.8	8.8	13.2	6.8	1.8	6.5	3	39.3	4.7
3	67/M	Mandible	II	5.0	5.4	18.5	2.1	2.4	4.1	2.4	2.3	4.5	1	27.6	0.2
4	37/F	Tongue	I	5.9	4.1	14.8	1.6	2.7	3.7	3.7	1.5	4.0	2	42.4	1.6
5	59/M	Tongue	II	7.3	11.7	48.0	3.1	2.5	5.1	2.4	4.8	9.3	1	48.7	1.5
6	73/M	Tongue	I	8.8	7.0	27.9	2.2	1.9	3.2	4.0	3.7	8.8	1	40.8	1.0
7	50/M	Tongue	II	14.6	9.3	51.4	2	1.2	1.7	7.3	8.1	29.8	2	46.2	2.4
8	75/F	Tongue	I	6.4	1.4	5.6	2.6	1.4	2.3	2.5	1.0	2.4	2	44.8	0.9
9	57/M	Floor of mouth	I	7.8	4.7	19.4	2.1	3.2	5.1	3.7	1.5	3.8	1	51.3	1.5
10	61/F	Tongue	I	7.8	2.1	8.9	1.8	1.0	1.5	4.3	2.0	5.8	2	21.1	0.2
11	66/F	Tongue	IVa	5.8	21.8	80.6	4.5	28.3	50.9	1.3	0.8	1.6	1	79.3	15.7
12	51/F	Mandible	I	5.1	8.2	28.7	1.6	1.3	1.7	3.2	6.3	17.1	2	18.6	0.1
13	50/M	Mandible	III	8.9	14.9	65.6	2.3	8.6	13.8	3.9	1.7	4.7	2	62.2	11.8
14	54/M	Tongue	II	10.6	15.9	71.7	4.2	12.8	25.6	2.5	1.2	2.8	3	82.7	6.1
15	66/F	Mandible	II	14.1	23.6	139.1	2.2	7.9	12.6	6.4	3.0	11.0	3	56.8	2.7
16	78/F	Mandible	III	15.8	6.9	149.5	3.7	11.6	24.3	4.3	0.6	6.2	2	67.0	9.9
17	81/F	Floor of mouth	IVa	13.3	15.5	93.1	3.1	7.3	14.5	4.3	2.1	6.4	2	64.1	3.8
18	65/F	Maxilla	II	11.7	57.1	342.6	3.4	35.9	71.8	3.4	1.6	4.8	2	52.3	16.1
19	79/F	Tongue	II	4.3	7.0	23.9	1.0	0.4	0.4	4.3	17.6	66.5	1	14.4	2.8
20	40/M	Buccal	IVa	16.2	13.9	79.5	5.8	17.7	42.4	2.8	0.8	1.9	1	87.6	5.9
21	65/F	Tongue	II	6.4	1.7	6.6	1.6	0.8	1.2	4.0	2.1	5.5	1	65.5	4.5
22	67/M	Mandible	IVa	14.0	55.2	320.2	8.7	35.8	89.5	1.6	1.5	3.6	2	54.1	14.9
23	31/M	Tongue	I	5.6	1.2	4.6	1.7	0.8	1.0	3.3	1.5	4.8	1	30.6	3.4
24	62/M	Tongue	I	3.5	0.5	1.6	1.8	0.5	0.8	1.9	1.0	2.1	1	11.6	0.1
25	65/F	Tongue	I	2.1	0.3	0.5	1.4	0.1	0.1	1.5	3.0	4.0	1	38.3	0.1

Tomiyoshi et al. (*20*). ^{18}F-FDG or ^{18}F-FAMT was administered intravenously at a dose of 5.0 MBq/kg after the patient had fasted for at least 6 h. PET was performed 64.0 ± 12.2 and 66.0 ± 14.0 min after administration for ^{18}F-FDG and ^{18}F-FAMT, respectively, using a PET/CT scanner (Discovery STE; GE Healthcare) with a 700-mm field of view and slice thickness of 3.27 mm. Three-dimensional data acquisition was done for 3 min per bed position, followed by the image reconstruction with the 3-dimensional ordered-subset expectation maximization method. The segmented attenuation correction was performed by CT (140 kV, 120–240 mAs) to produce 128 × 128 matrix images.

All patients underwent ^{18}F-FDG PET imaging first and then continued with ^{18}F-FAMT PET before surgery. One of 3 experienced nuclear medicine physicians (minimum 5 y experience in general nuclear medicine and 4 y in PET/CT) interpreted each PET image of ^{18}F-FAMT and ^{18}F-FDG. The PET images were first examined visually for abnormal ^{18}F-FDG or ^{18}F-FAMT accumulation, and regions of interest covering the whole tumor were placed manually over every axial image plane, to obtain SUV_{max} for a semiquantitative analysis of tumor uptake.

PET tumor volumes were calculated using PET volume computerized-assisted reporting, an automated segmentation software (Advantage Workstation; GE Healthcare). With a predetermined pathologically confirmed cutoff SUV of 3.0 for ^{18}F-FDG and 1.4 for ^{18}F-FAMT from previous PET study of maxillofacial tumors (*19*), PET volume computerized-assisted reporting performs autosegmentation to the threshold-defined volumes and automatically calculates MTV and average SUV (*10*). TLG of ^{18}F-FDG was calculated by multiplying MTV with the average SUV within that volume. A similar formula was used to determine TLR of ^{18}F-FAMT. TLR is defined as a parameter similar to TLG and describes the quantitative amount of ^{18}F-FAMT trapped in tumor cells. For semiquantitative comparison, ^{18}F-FDG–to–^{18}F-FAMT ratios of SUV_{max}, MTV, and TLG/TLR were calculated.

Tumor Histopathologic Analysis

The surgical specimens were fixed in 10% formalin solution, paraffin-embedded, decalcified when needed overnight, and sectioned (3 μm) for pathologic and immunohistochemical analysis. Pathologic tumor volume (PTV) is measured 3-dimensionally using the length (l), width (w), and thickness (t) by the classic formula $(\pi/6) \times l \times w \times t$.

Hematoxylin and eosin (H-E) staining was performed for inflammation analysis. A 4-grade classification of inflammation was used on the basis of the distribution of inflammatory cells within the tumor tissue and its surroundings (Table 1) (*21*). Tumor with an inflammation grade of 2 and 3 was considered to have a severe inflammation, whereas grade 0 and 1 were similar to normal organs. Immunohistochemical staining was performed using the labeled streptavidin biotinylated antibody method (*14*). Molecular immunology borstel-1 or MIB-1 (Dako), a murine monoclonal antibody specific for human nuclear antigen Ki-67, was used in a 1:100 dilution.

Statistical Analysis

Nonparametric tests (Spearman rank test and Mann–Whitney U test) were used to determine the statistical difference of variables. Relationships within variables were measured using Pearson correlation analysis. For both radiotracers' MTV, further analysis with the Bland–Altman method was used to determine the degree of agreement of the MTVs with PTVs. Probability values of less than 0.05 indicated a statistically significant difference. Results were shown as mean ± SD.

RESULTS

Patients

The average time interval from the last ^{18}F-FDG PET to ^{18}F-FAMT PET was 9.8 ± 10.8 d (range, 2–56 d), and the average time interval from ^{18}F-FAMT PET studies to surgery was 16.7 ± 10.1 d. All patients' characteristics, their tumor PET quantitative values, tumor volumes, and Ki-67 LIs are summarized in Table 2. Inflammations were found in all patients' tumors.

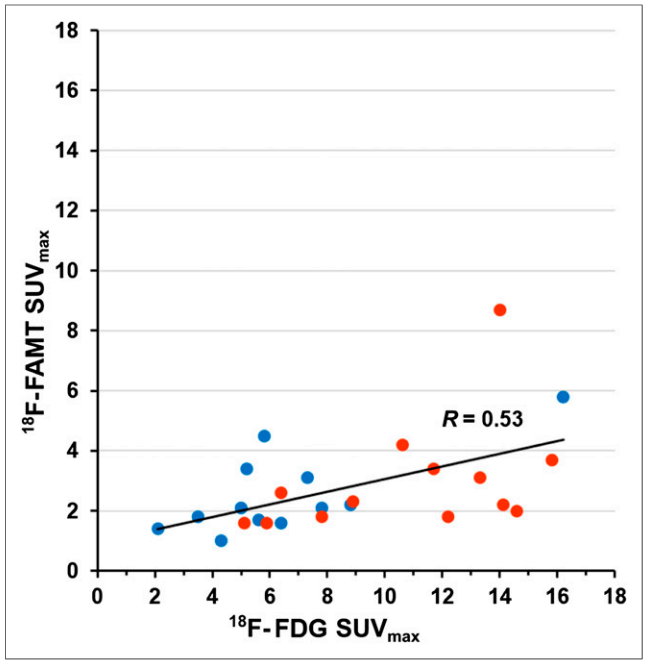

FIGURE 1. Correlation analysis of SUV_{max} of ^{18}F-FDG and ^{18}F-FAMT.

Inflammation Involvement in PET Images and Histologic Sections

The high ^{18}F-FDG SUV_{max} without correspondingly high ^{18}F-FAMT SUV_{max} is shown on the right lower quadrant of the Pearson correlation graph in Figure 1 (R = 0.53, P = 0.003). This tendency is further described in Figure 2A, in which the ^{18}F-FDG–to–^{18}F-FAMT SUV_{max} ratio is significantly higher in the grade 2 and 3 group (P = 0.030), showing that high SUV_{max} of ^{18}F-FDG was significantly correlated with advanced tumor inflammation.

In contrast, the ^{18}F-FDG–to–^{18}F-FAMT ratio of MTV and TLG/TLR showed no difference between inflammation groups (Fig. 2B, P = 0.76; Fig. 2C, P = 0.10, respectively). However, some outliers were observed and suggest more cautious interpretation.

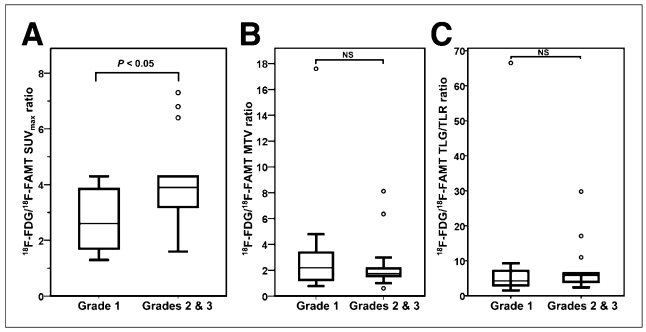

FIGURE 2. ^{18}F-FDG–to–^{18}F-FAMT ratio of PET parameters. (A) ^{18}F-FDG–to–^{18}F-FAMT SUV_{max} ratio is significantly higher on tumor with high inflammation grade. (B and C) PET metabolic parameters (MTV [B] and TLG/TLR [C]) showed that ^{18}F-FDG and ^{18}F-FAMT are similar when uptake is calculated from whole tumor. NS = not significant.

TABLE 3
Spearman Rank Correlation Coefficients for All PET Parameters, Ki-67, and PTV

			^{18}F-FDG			^{18}F-FAMT			
		Ki-67	SUV_{max}	MTV	TLG	SUV_{max}	MTV	TLR	PTV (cm^3)
Ki-67		1.0000							
^{18}F-FDG	SUV_{max}	0.6749*	1.0000						
	MTV	0.5462*	0.5975*	1.0000					
	TLG	0.6192*	0.7511*	0.9169*	1.0000				
^{18}F-FAMT	SUV_{max}	0.7039*	0.5783*	0.6388*	0.6935*	1.0000			
	MTV	0.7182*	0.6506*	0.8140*	0.8602*	0.8305*	1.0000		
	TLR*	0.7477*	0.6653*	0.8254*	0.8731*	0.8770*	0.9890*	1.0000	
PTV (cm^3)		0.7454*	0.6114*	0.6769*	0.7277*	0.5486*	0.7386*	0.7362*	1.0000

*$P < 0.01$.
All correlations were calculated using independent data points from 25 patients.

Spearman rank correlation coefficients showed that Ki-67 LI correlated with all PET parameters (Table 3). Even though SUV_{max} of both radiotracers correlates with Ki-67, in ^{18}F-FAMT, correlation coefficients of MTV and TLR were $\rho = 0.718$ and 0.748, whereas, in ^{18}F-FDG, correlation coefficients of MTV and TLG were lower, $\rho = 0.546$ and 0.619, respectively. The SUV_{max} of ^{18}F-FDG and ^{18}F-FAMT were only moderately correlated with each other ($\rho = 0.578$), whereas their MTV and TLG/TLR were strongly correlated ($\rho = 0.814$ and 0.873, respectively).

The potentials of MTV to predict the actual tumor volume using of both radiotracers were evaluated by direct comparisons with PTV. MTV values of ^{18}F-FAMT and ^{18}F-FDG provided a good estimation of the actual tumor volume (Fig. 3A, $R = 0.77$ and 0.90, respectively). Bland–Altman analysis (Fig. 3B) further demonstrated that tumor volumes measured by the MTV of ^{18}F-FAMT showed better agreement with actual tumor volume (bias = 3.4 ± 6.42 cm^3, 95% confidence interval = 0.77–6.09 cm^3) than that of ^{18}F-FDG MTV (bias = 8.1 ± 11.7 cm^3, 95% confidence interval = 3.45–12.67 cm^3).

Case Figures

A representative case presented in Figure 4 (patient 20) shows that both ^{18}F-FDG and ^{18}F-FAMT SUV_{max} parameters demonstrate high uptake. Ki-67 LI from the pathologic specimen was also high (87.6%). However, H-E staining showed that inflammation in this tumor was minimal.

A discordant SUV_{max} finding between ^{18}F-FDG and ^{18}F-FAMT (patient 2) is presented in Figure 5. In this case, low uptake of ^{18}F-FAMT was suggestive for low tumor activity, as confirmed by a low Ki-67 LI. However, the tumor stage of this patient was advanced due to the presence of neck lymph node metastasis (also confirmed by ^{18}F-FAMT uptake). H-E staining revealed that this tumor had high-grade inflammatory cell infiltration in the invasion area and consisted of mainly neutrophil granulocyte.

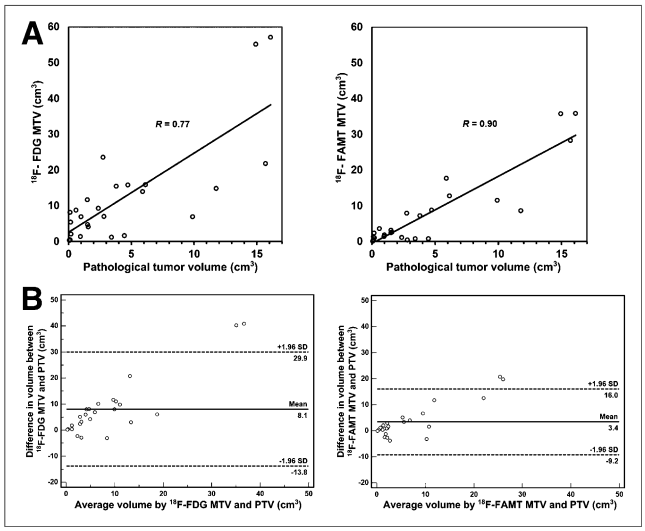

FIGURE 3. (A) Prediction of actual tumor volume using MTV of ^{18}F-FDG and ^{18}F-FAMT. (B) Bland–Altman analysis. ^{18}F-FAMT MTV predicts tumor size more accurately.

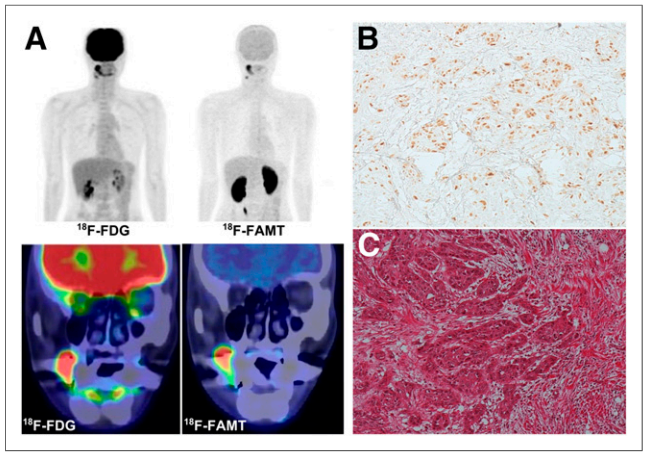

FIGURE 4. A 40-y-old man with OSCC in right buccal region. (A) Mean-intensity-projection and coronal images of ^{18}F-FDG and ^{18}F-FAMT PET of primary lesion. High ^{18}F-FDG and ^{18}F-FAMT tumor uptake was noted. Concordant high uptake of ^{18}F-FDG ($SUV_{max} = 16.2$) and ^{18}F-FAMT ($SUV_{max} = 5.8$) was also noted. A high Ki-67 LI value (87.6%) is shown in immunohistochemistry sections (B), and H-E staining showed grade 1 tumor inflammation (C).

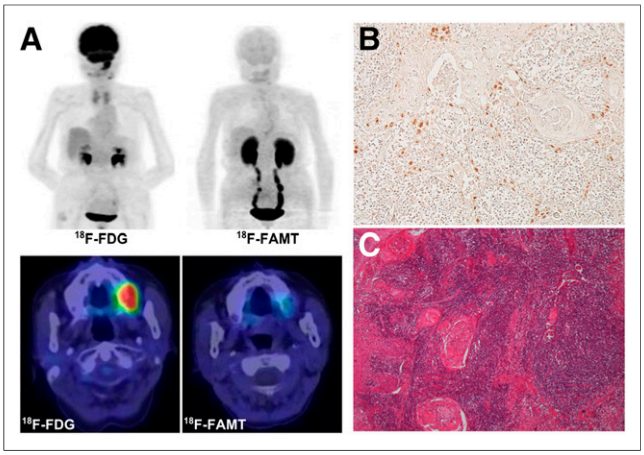

FIGURE 5. An 88-y-old woman with OSCC in left maxilla region. (A) Mean-intensity-projection and axial images of ^{18}F-FDG and ^{18}F-FAMT PET of primary lesion. High ^{18}F-FDG uptake (SUV_{max} = 12.2) is noted while on same plane, ^{18}F-FAMT uptake (SUV_{max} = 1.8) is low. Low tumor proliferation activity is shown by low Ki-67 LI value (39.3%) (B), whereas H-E staining showed grade 3 tumor inflammation (C).

In these 2 patients, all ^{18}F-FAMT parameters corresponded well with Ki-67 staining and PTV. Besides patient 2, 2 other patients (patients 7 and 15) had extremely high ^{18}F-FDG SUV_{max} without evidence of appropriate PTV, and interestingly their ^{18}F-FAMT parameters matched with their tumor size and proliferation.

DISCUSSION

^{18}F-FDG is the most widely used PET radiotracer for malignancies (*22*). As a glucose analog, ^{18}F-FDG accumulates in the cells through glucose transporter-1 receptors; these receptors are highly expressed in most malignant cells because of their high metabolic activity. However, active nonmalignant pathologic processes, such as inflammation and infection, may also enhance glycolytic metabolism. Although it has been reported that inflammatory tumors might complicate ^{18}F-FDG PET analysis, this concept has not been validated (*23*).

We demonstrated that the SUV_{max} of ^{18}F-FDG and ^{18}F-FAMT were only moderately correlated. Given that ^{18}F-FAMT is more tumor-specific, this finding prompted us to analyze further the inflammation involvement. A significantly higher ^{18}F-FDG–to–^{18}F-FAMT SUV_{max} ratio in inflammatory tumor strongly suggested that ^{18}F-FDG SUV_{max} was largely influenced by the intratumoral inflammatory process.

Inflammation is an integral part of the natural course of OSCC carcinogenesis. The highly diverse surfaces in the oral cavity provide a milieu for more than 750 distinct taxa of bacteria. Thus, the oral epithelium is constantly exposed to external challenges at both the cellular and the molecular levels. The evidence suggests that there is a link between microbial infection and OSCC (*24*).

Tumor cell proliferation rate is reported as a prognostic factor in head and neck carcinomas (*25*). In oral cavity epidermoid carcinomas, Ki-67 expression serves as an independent prognostic factor for survival (*26*). However, it is impossible to obtain comprehensive Ki-67 status because of the invasive nature of the biopsy. Thus, developing methods to evaluate cell proliferation activity from PET images would certainly be beneficial (*27,28*). Regarding the nature of ^{18}F-FDG, such an objective could only be optimally accomplished using a more malignant-specific radiotracer.

The SUV_{max} of ^{18}F-FDG PET provides prognostic information additional to that provided by the American Joint Committee on Cancer stage (*18*) and data useful for tumor-aggressiveness evaluation, early detection of recurrence, and outcome prediction in head and neck cancers (*16,18*). Despite its popularity and practical application, however, SUV_{max} is derived only from a single pixel, thus it may not represent the whole tumor entity and does not provide any information regarding tumor biology (*29,30*). Furthermore, SUV_{max} is highly sensitive to noise and affected by the partial-volume effect (*30,31*). These phenomena appear particularly in inflammatory lesions; therefore, the evaluation of biologic and anatomic tumor data based only on SUV_{max} is highly susceptible to bias (*30*).

Nowadays, advanced image analysis tools and 3-dimensional display techniques allow quick and consistent volume-based assessment. Recently, new ^{18}F-FDG PET parameters (MTV and TLG) have been introduced and showed their potential as an alternative to SUV_{max} by offering more relevant tumor information while combining both metabolic activity and 3-dimensional tumor volume (*15,16*). In lung cancer, recently these parameters served as significant prognostic factors for survival and provided better prognostic imaging biomarkers than SUV_{max} (*31*). In OSCC, TLG was suspected to be also reliable as an independent prognostic factor for recurrence and metastasis. In head and neck cancer, adding primary tumor TLG into a prognostic scoring system might be useful for risk stratification (*15*). Together, ^{18}F-FDG MTV and TLG provide such potential in OSCC treated with chemoradiotherapy (*32*). Moreover, in a recent systematic review, both parameters are accurate prognostic indicators of outcome in head and neck cancer (*33*).

In this study, we evaluated the potential of ^{18}F-FAMT and these new PET parameters for accurate depiction of both biologic and anatomic profiles of oral tumors. The potential of L-type amino acid transporter 1 as a therapeutic target in oral cancer has been described long before (*34,35*). We designed ^{18}F-FAMT as a specific PET radiotracer for L-type amino acid transporter 1 that is overexpressed exclusively in malignant tumors (*12*) and performed several clinical trials in comparison with ^{18}F-FDG in oral malignancies (*10,14,19*). Therefore, analysis of ^{18}F-FAMT and its corresponding tumor pathologic characteristics is fundamental for the development of a PET imaging–based comprehensive diagnosis of tumor growth.

Previously, we reported that SUV_{max} of ^{18}F-FAMT PET images showed better correlation with Ki-67 expression and clinicopathologic variables than ^{18}F-FDG in the primary tumor of OSCC (*14*). Our current study elaborated this finding by introducing new parameters in the evaluation of both PET radiotracers. Consistent with the previous report, all ^{18}F-FAMT parameters surpassed those of ^{18}F-FDG in providing better correlation with cell proliferation activity. In particular, the MTV and TLR of ^{18}F-FAMT showed their potential as an SUV_{max} replacement, because they have a stronger correlation with cell proliferation activity, compared with SUV_{max}. Such findings were not observed in ^{18}F-FDG, for which both new parameters correlated less well with Ki-67, showing that ^{18}F-FAMT is superior to ^{18}F-FDG in its accuracy to predict tumor cell growth in OSCC.

The correlation between ^{18}F-FAMT's new parameters and Ki-67 in this study revealed the potential of ^{18}F-FAMT for use as a predictor of tumor cell growth in OSCC. The specificity of ^{18}F-FAMT for malignant and highly proliferating tumors is shown in Figure 4 (patient 20); the SUV_{max} for both ^{18}F-FDG and ^{18}F-FAMT corresponded well to the radiotracer's high expression of tumor Ki-67. As shown in Figure 5 (patient 2), the expression of Ki-67 correlated well with ^{18}F-FAMT uptake, whereas ^{18}F-FDG showed a high

uptake suggestive of a false-positive result caused by inflammation or nonspecific uptake, which is prone to overestimation.

If we may further hypothesize by taking into account the well-established correlation between Ki-67 and patients' survival, our findings suggest that ^{18}F-FAMT and its new parameters might provide immediate predictions of patients' survival, through the estimation of tumor cell proliferation. This relationship is currently under evaluation.

This study is limited by the use of pathologically confirmed fixed SUV cutoff values for the segmentation threshold, which is exclusive for OSCC. Gradient-based segmentation might be a better method for other tumors than the fixed-threshold method; however, similar results were not observed in head and neck cancers (*18,36*). Finally, this was a retrospective single-center study, thus the results might be subject to selection bias. In general, further investigations are needed to elucidate the effects of the intratumoral inflammatory process on ^{18}F-FDG uptake in other types of tumors.

CONCLUSION

^{18}F-FDG uptake was overestimated by additional uptake related to the intratumoral inflammatory process, whereas ^{18}F-FAMT simply accumulated in tumors according to tumor activity as evaluated by Ki-67 LI.

DISCLOSURE

The costs of publication of this article were defrayed in part by the payment of page charges. Therefore, and solely to indicate this fact, this article is hereby marked "advertisement" in accordance with 18 USC section 1734. No potential conflict of interest relevant to this article was reported.

REFERENCES

1. Jemal A, Bray F, Center MM, Ferlay J, Ward E, Forman D. Global cancer statistics. *CA Cancer J Clin.* 2011;61:69–90.
2. Cooper JS, Porter K, Mallin K, et al. National Cancer Database report on cancer of the head and neck: 10-year update. *Head Neck.* 2009;31:748–758.
3. Zini A, Czerninski R, Sgan-Cohen HD. Oral cancer over four decades: epidemiology, trends, histology, and survival by anatomical sites. *J Oral Pathol Med.* 2010;39:299–305.
4. Lonneux M, Hamoir M, Reychler H, et al. Positron emission tomography with [^{18}F]fluorodeoxyglucose improves staging and patient management in patients with head and neck squamous cell carcinoma: a multicenter prospective study. *J Clin Oncol.* 2010;28:1190–1195.
5. Senft A, de Bree R, Hoekstra OS, et al. Screening for distant metastases in head and neck cancer patients by chest CT or whole body FDG-PET: a prospective multicenter trial. *Radiother Oncol.* 2008;87:221–229.
6. Xie P, Li M, Zhao H, Sun X, Fu Z, Yu J. ^{18}F-FDG PET or PET-CT to evaluate prognosis for head and neck cancer: a meta-analysis. *J Cancer Res Clin Oncol.* 2011;137:1085–1093.
7. Burger IA, Huser DM, Burger C, von Schulthess GK, Buck A. Repeatability of FDG quantification in tumor imaging: averaged SUVs are superior to SUVmax. *Nucl Med Biol.* 2012;39:666–670.
8. Wahl RL, Jacene H, Kasamon Y, Lodge MA. From RECIST to PERCIST: evolving considerations for PET response criteria in solid tumors. *J Nucl Med.* 2009;50(suppl 1):122S–150S.
9. van den Hoff J, Oehme L, Schramm G, et al. The PET-derived tumor-to-blood standard uptake ratio (SUR) is superior to tumor SUV as a surrogate parameter of the metabolic rate of FDG. *EJNMMI Res.* 2013;3:77.
10. Kim M, Higuchi T, Arisaka Y, et al. Clinical significance of ^{18}F-α-methyl tyrosine PET/CT for the detection of bone marrow invasion in patients with oral squamous cell carcinoma: comparison with ^{18}F-FDG PET/CT and MRI. *Ann Nucl Med.* 2013;27:423–430.
11. Nobusawa A, Kim M, Kaira K, et al. Diagnostic usefulness of ^{18}F-FAMT PET and L-type amino acid transporter 1 (LAT1) expression in oral squamous cell carcinoma. *Eur J Nucl Med Mol Imaging.* 2013;40:1692–1700.
12. Wiriyasermkul P, Nagamori S, Tominaga H, et al. Transport of 3-fluoro-L-α-methyl-tyrosine by tumor-upregulated L-type amino acid transporter 1: a cause of the tumor uptake in PET. *J Nucl Med.* 2012;53:1253–1261.
13. Jacob R, Welkoborsky HJ, Mann WJ, Jauch M, Amedee R. [Fluorine-18] fluorodeoxyglucose positron emission tomography, DNA ploidy and growth fraction in squamous-cell carcinomas of the head and neck. *ORL J Otorhinolaryngol Relat Spec.* 2001;63:307–313.
14. Miyashita G, Higuchi T, Oriuchi N, et al. ^{18}F-FAMT uptake correlates with tumor proliferative activity in oral squamous cell carcinoma: comparative study with ^{18}F-FDG PET and immunohistochemistry. *Ann Nucl Med.* 2010;24:579–584.
15. Abd El-Hafez YG, Moustafa HM, Khalil HF, Liao CT, Yen TC. Total lesion glycolysis: a possible new prognostic parameter in oral cavity squamous cell carcinoma. *Oral Oncol.* 2013;49:261–268.
16. Chan SC, Hsu CL, Yen TC, Ng SH, Liao CT, Wang HM. The role of ^{18}F-FDG PET/CT metabolic tumour volume in predicting survival in patients with metastatic nasopharyngeal carcinoma. *Oral Oncol.* 2013;49:71–78.
17. Quon A, Fischbein NJ, McDougall IR, et al. Clinical role of ^{18}F-FDG PET/CT in the management of squamous cell carcinoma of the head and neck and thyroid carcinoma. *J Nucl Med.* 2007;48(suppl 1):58S–67S.
18. Dibble EH, Alvarez AC, Truong MT, Mercier G, Cook EF, Subramaniam RM. ^{18}F-FDG metabolic tumor volume and total glycolytic activity of oral cavity and oropharyngeal squamous cell cancer: adding value to clinical staging. *J Nucl Med.* 2012;53:709–715.
19. Miyakubo M, Oriuchi N, Tsushima Y, et al. Diagnosis of maxillofacial tumor with L-3-[^{18}F]-fluoro-alpha-methyltyrosine (FMT) PET: a comparative study with FDG-PET. *Ann Nucl Med.* 2007;21:129–135.
20. Tomiyoshi K, Amed K, Muhammad S, et al. Synthesis of isomers of ^{18}F-labelled amino acid radiopharmaceutical: position 2- and 3-L-^{18}F-α-methyltyrosine using a separation and purification system. *Nucl Med Commun.* 1997;18:169–175.
21. Klintrup K, Makinen JM, Kauppila S, et al. Inflammation and prognosis in colorectal cancer. *Eur J Cancer.* 2005;41:2645–2654.
22. Kunkel M, Forster GJ, Reichert TE, et al. Detection of recurrent oral squamous cell carcinoma by [^{18}F]-2-fluorodeoxyglucose-positron emission tomography: implications for prognosis and patient management. *Cancer.* 2003;98:2257–2265.
23. Culverwell AD, Scarsbrook AF, Chowdhury FU. False-positive uptake on 2-[^{18}F]-fluoro-2-deoxy-D-glucose (FDG) positron-emission tomography/computed tomography (PET/CT) in oncological imaging. *Clin Radiol.* 2011;66:366–382.
24. Hooper SJ, Wilson MJ, Crean SJ. Exploring the link between microorganisms and oral cancer: a systematic review of the literature. *Head Neck.* 2009;31:1228–1239.
25. Thomas B, Stedman M, Davies L. Grade as a prognostic factor in oral squamous cell carcinoma: a population-based analysis of the data. *Laryngoscope.* 2014;124:688–694.
26. Motta RR, Zettler CG, Cambruzzi E, Jotz GP, Berni RB. Ki-67 and p53 correlation prognostic value in squamous cell carcinomas of the oral cavity and tongue. *Braz J Otorhinolaryngol.* 2009;75:544–549.
27. Kurokawa H, Zhang M, Matsumoto S, et al. The relationship of the histologic grade at the deep invasive front and the expression of Ki-67 antigen and p53 protein in oral squamous cell carcinoma. *J Oral Pathol Med.* 2005;34:602–607.
28. Myoung H, Kim MJ, Lee JH, Ok YJ, Paeng JY, Yun PY. Correlation of proliferative markers (Ki-67 and PCNA) with survival and lymph node metastasis in oral squamous cell carcinoma: a clinical and histopathological analysis of 113 patients. *Int J Oral Maxillofac Surg.* 2006;35:1005–1010.
29. Murphy JD, Chisholm KM, Daly ME, et al. Correlation between metabolic tumor volume and pathologic tumor volume in squamous cell carcinoma of the oral cavity. *Radiother Oncol.* 2011;101:356–361.
30. Soret M, Bacharach SL, Buvat I. Partial-volume effect in PET tumor imaging. *J Nucl Med.* 2007;48:932–945.
31. Hyun SH, Ahn HK, Kim H, et al. Volume-based assessment by ^{18}F-FDG PET/CT predicts survival in patients with stage III non-small-cell lung cancer. *Eur J Nucl Med Mol Imaging.* 2014;41:50–58.
32. Lim R, Eaton A, Lee NY, et al. ^{18}F-FDG PET/CT metabolic tumor volume and total lesion glycolysis predict outcome in oropharyngeal squamous cell carcinoma. *J Nucl Med.* 2012;53:1506–1513.
33. Pak K, Cheon GJ, Nam HY, et al. Prognostic value of metabolic tumor volume and total lesion glycolysis in head and neck cancer: a systematic review and meta-analysis. *J Nucl Med.* 2014;55:884–890.
34. Kim CH, Park KJ, Park JR, et al. The RNA interference of amino acid transporter LAT1 inhibits the growth of KB human oral cancer cells. *Anticancer Res.* 2006;26:2943–2948.
35. Kim DK, Ahn SG, Park JC, Kanai Y, Endou H, Yoon JH. Expression of L-type amino acid transporter 1 (LAT1) and 4F2 heavy chain (4F2hc) in oral squamous cell carcinoma and its precursor lesions. *Anticancer Res.* 2004;24:1671–1675.
36. Sridhar P, Mercier G, Tan J, Truong MT, Daly B, Subramaniam RM. FDG PET metabolic tumor volume segmentation and pathologic volume of primary human solid tumors. *AJR.* 2014;202:1114–1119.